Arch Appl Mech (2009) 79: 499–508
DOI 10.1007/s00419-008-0284-8

SPECIAL ISSUE

Czesław I. Bajer · Bartłomiej Dyniewicz

Numerical modelling of structure vibrations under inertial moving load

Received: 6 January 2008 / Accepted: 24 September 2008 / Published online: 10 January 2009
© Springer-Verlag 2008

Abstract Inertial loading of structures by mass travelling with near-critical velocity has been intensively debated. In the literature a moving mass is replaced by an equivalent force or an oscillator that is in permanent contact with the structure. A direct mass matrix modification method frequently implemented in the finite element approach gives reasonable results only in the range of relatively low velocities and for low mass value if compared with the mass of a structure. However, existing solutions are incorrect and are not implemented in commercial computer codes. In this paper we present the space–time finite element approach to the problem. The interaction of the moving mass/supporting structure is described in a local coordinate system of the space-time finite element domain. Resulting characteristic matrices include inertia, Coriolis and centrifugal forces. Simple modification of matrices in the discrete equations of motion allows us to gain accuracy in a wide range of velocity, up to the over-critical speed. Numerical examples of string and beam vibrations prove the simplicity and efficiency of the method.

Keywords Moving mass · Inertial load · Space–time finite element method · Vibrations

1 Introduction

Inertial loads moving on strings, beams and plates with sub or super critical velocities are especially important for engineers. Theoretical and numerical solutions are applied to problems with single or multi-point contact such as train–track or vehicle–bridge interaction, pantograph collectors in railways, magnetic railways, guideways in robotic technology, etc.

First, the difference between the inertial loading and loading by moving massless force must be emphasised. In the inertial load problem the moving mass is placed directly on the structure while the massless force represents only the equivalent inertia influence or is modelled as a spring-mass system load. Both applications do not result in proper displacements and mass trajectory. The present paper deals with the first type of loading. In common practice, differential equations derived for moving mass problems are solved numerically by using of finite element techniques. However, this approach has considerable disadvantages. As long as mass influence is considered as an equivalent force system, computations can be performed with sufficient accuracy only in low range of the speed (in the case of a string up to 0.2–0.3 of the wave speed and for low mass values). The solution, however, is still incorrect. The analysis of the string vibrations performed according to [1] is divergent (Fig. 1). In the case of a beam the divergence rate is lower than for a string, because of the different type of the differential equation. We must emphasize here that traditional finite element method fails since it does not allow

C. I. Bajer (✉) · B. Dyniewicz
Institute of Fundamental Technological Research, Polish Academy of Sciences, Świętokrzyska 21, 00-049 Warsaw, Poland
E-mail: cbajer@ippt.gov.pl; cbajer@chello.pl

B. Dyniewicz
E-mail: bdynie@ippt.gov.pl

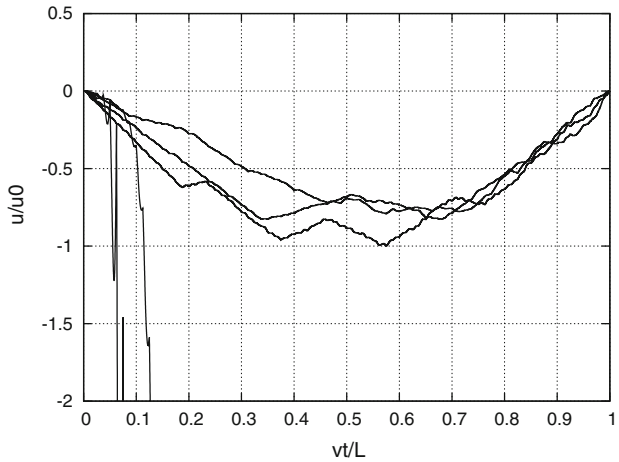

Fig. 1 Divergency of the existing numerical solution

the precise discretization of the differential equation in the interval between two successive whiles. The space-time finite element method has no such limitation. In the space-time approach the equation in the whole time interval in discrete time is being considered. The space-time element method can be considered as the extension of the traditional finite element method in the time domain [2]. Non-stationary partition of the structure and non rectangular space-time elements [3,4] enabled the solving of a new group of problems by the space-time element method: problems with adaptive mesh [5–7], contact problems [8,9], large deformations [10].

In this paper we discuss the numerical aspects of the moving mass, placed directly on the structure. The influence of the moving force alone is trivial and this question will not be considered. The moving mass cannot be simply incorporated in the discrete formulation. The space-time formulation is used to derive matrices which contribute to moving mass effect. Consequent formulation results in a proper time stepping scheme. The space-time finite element formulation seems to be the best, and unique so far, approach to formulate the problem and to derive respective characteristic matrices of the step-by-step procedure of time integration of the motion equation.

The analysis of the moving mass problem is widely presented in literature. The closed solution exists only in the case of mass moving on a massless string [11,12]. Otherwise, final results are obtained numerically, although the solution is preceded by complex analytical calculations. In numerous references authors treat the problem in a low range of the mass speed. In such a case results are sufficiently good, even if the inertial term contributing to moving mass is not correctly treated by the time integration method. Simply, the moving mass influence in such cases is minor compared with static displacements.

Measurements of the wave speed in railway tracks treated as beams show values between 800 and 1000 km/h. In the case of soaked ground the speed can decrease to 500 km/h or less. Dynamic influence of the moving load significantly increases the structure deflection. The highest dynamic contribution determines the critical speed of motion. Practically, the critical mass speed equals 0.4–0.5 of the wave speed. This is the range of the speed of the modern vehicle.

The dynamic problem is considered as a sequence of static solutions, performed step-by-step with a prescribed time increment. At a low velocity of the mass (approximately up to 0.1 of the critical speed and up to 0.2 of the wave speed in the unloaded and unballasted structure), simple replacement of the mass from joint to joint or from element to element can be applied with an error sufficiently low for engineering purposes. However, the error dramatically increases with the increase of the travelling speed and such an approach cannot be applied to a general case. Direct modification of global characteristic matrices in the discrete system is attractive since it allows us to avoid computational complexity as in the case of moving oscillators or the imposition of supplementary constraints.

2 Formulation of the problem

Let us consider a string of the length l, cross-sectional area A, mass density ρ, tensile force N, subjected to a concentrated mass m accompanied by a point force P (Fig. 2), moving with a constant speed v_m. The motion

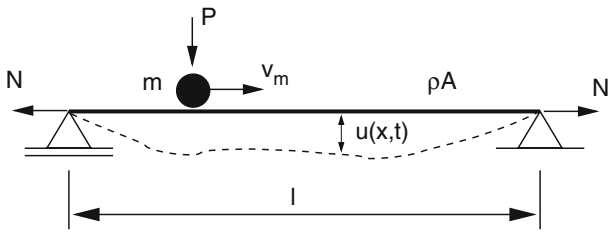

Fig. 2 Moving inertial load

equation of the string under the moving inertial load has a form

$$-N\,\frac{\partial^2 u(x,t)}{\partial x^2}\;+\;\rho A\,\frac{\partial^2 u(x,t)}{\partial t^2}\;=\;\delta(x-v_m t)P\;-\;\delta(x-v_m t)m\,\frac{\mathrm{d}^2 u(v_m t,t)}{\mathrm{d}t^2}. \tag{1}$$

We impose initial conditions $u(x,0)=0, \partial u(x,t)/\partial t\Big|_{t=0}=0$ and boundary conditions $u(0,t)=0,\ u(l,t)=0$.

The problem can easily be solved analytically or numerically if P is the only travelling factor and $m=0$. Respective closed solutions or series expansions exist in such a case. However, in our paper we concentrate on the influence of the inertial moving term. We consider small displacements of the string.

2.1 Theoretical analysis

The general semi-analytical solution is given below for two reasons. First, we use it as a reference solution to be compared with numerical results. Second, we intend to emphasize discontinuity of the mass trajectory at the end support. This important property is visible both in semi-analytical and numerical results and influences the response of more complex systems. Moreover, it is mathematically proved in [13,14]. The final solution is obtained as a matrix differential equation of the second order. Numerical integration results in the solution valid in a full range of the velocity. We can mention here that exactly the same approach can be applied to a beam with a moving mass.

In order to reduce a partial differential equation to the ordinary differential equation, we apply the Fourier sine integral transformation in a finite range $\langle 0, l\rangle$

$$V(j,t)\;=\;\int_0^l u(x,t)\,\sin\frac{j\pi x}{l}\,\mathrm{d}x\quad u(x,t)\;=\;\frac{2}{l}\sum_{j=1}^{\infty}V(j,t)\,\sin\frac{j\pi x}{l}. \tag{2}$$

The motion equation after the Fourier transformation is in the following form

$$\begin{aligned}&\ddot{V}(j,t)\;+\;\alpha\sum_{k=1}^{\infty}\ddot{V}(k,t)\,\sin\omega_k t\,\sin\omega_j t\;+\;2\alpha\sum_{k=1}^{\infty}\omega_k\,\dot{V}(k,t)\,\cos\omega_k t\,\sin\omega_j t\\&+\;\Omega^2\,V(j,t)\;-\;\alpha\sum_{k=1}^{\infty}\omega_k^2\,V(k,t)\,\sin\omega_k t\,\sin\omega_j t\;=\;\frac{P}{\rho A}\,\sin\omega_j t,\end{aligned} \tag{3}$$

where

$$\omega_k\;=\;\frac{k\pi v_m}{l},\quad \omega_j\;=\;\frac{j\pi v_m}{l},\quad \Omega^2\;=\;\frac{N}{\rho A}\,\frac{j^2\pi^2}{l^2},\quad \alpha\;=\;\frac{2m}{\rho A\,l}. \tag{4}$$

The analytical solution to this problem is unknown. We must solve this equation numerically. The Eq. (3) can be written in a matrix form, where matrices **M**, **C** and **K** are square matrices ($j, k = 1...n$)

$$\mathbf{M}\ddot{\mathbf{V}} + \mathbf{C}\dot{\mathbf{V}} + \mathbf{K}\mathbf{V} = \mathbf{P}, \tag{5}$$

where matrices' elements are as follows:

$$m_{ij} = \alpha \sin\frac{i\pi v_m t}{l} \sin\frac{j\pi v_m t}{l} + \delta_{ij}, \tag{6}$$

$$c_{ij} = 2\alpha\frac{j\pi v_m t}{l} \sin\frac{i\pi v_m t}{l} \cos\frac{j\pi v_m t}{l}, \tag{7}$$

$$k_{ij} = \frac{i^2\pi^2}{l^2}\frac{N}{\rho A}\delta_{ij} - \alpha\frac{j^2\pi^2 v_m^2}{l^2} \sin\frac{i\pi v_m t}{l} \sin\frac{j\pi v_m t}{l}, \tag{8}$$

and vector elements

$$p_i = \frac{P}{\rho A} \sin\frac{i\pi v_m t}{l}, \tag{9}$$

where $v_i = V(i, t)$ and δ_{ij} is the Kronecker delta. When coefficients $V(j, t)$ are computed, displacements of the string (2) constitute the solution of (1). The solution is determined in a full range of v_m. We can calculate displacement in each point of string and for all values of v_m.

2.2 Results of semi-analytical calculations

The integration of the Eq. (5) results in components which describe displacements in time (2). Fig. 3 presents the mass trajectories for the dimensionless velocities of the range 0.1–1.0.

The analysis of results exhibits a jump of the mass in the neighbourhood of the end support. In the papers [13,14] the discontinuity of the mass trajectory near the end support was mathematically proved. The proof was given in the case of massless string. This solution enabled us to prove the jump of the trajectory in the whole range of the speed $0 < v_m \leq c$. The conclusion is important for further numerical investigations and final conclusions. What is more, this exhibited property results in significant inconveniences in discrete solutions.

In the case of inertial string the pure mathematical proof cannot be given. Numerical integration of the second order differential Eq. (5) results in a discontinuity of the mass trajectory. Especially for $v_m = 0.5c$, the moving mass approaches the end support in a phase of deep vertical displacement. In spite of low convergence of the sum (2) good accuracy of results was obtained.

A global analytical solution can be considered as a reference solution. Although it is valid for the whole range of the speed v_m (sub-critical, critical and over-critical), it can be used in a limited range of engineering problems.

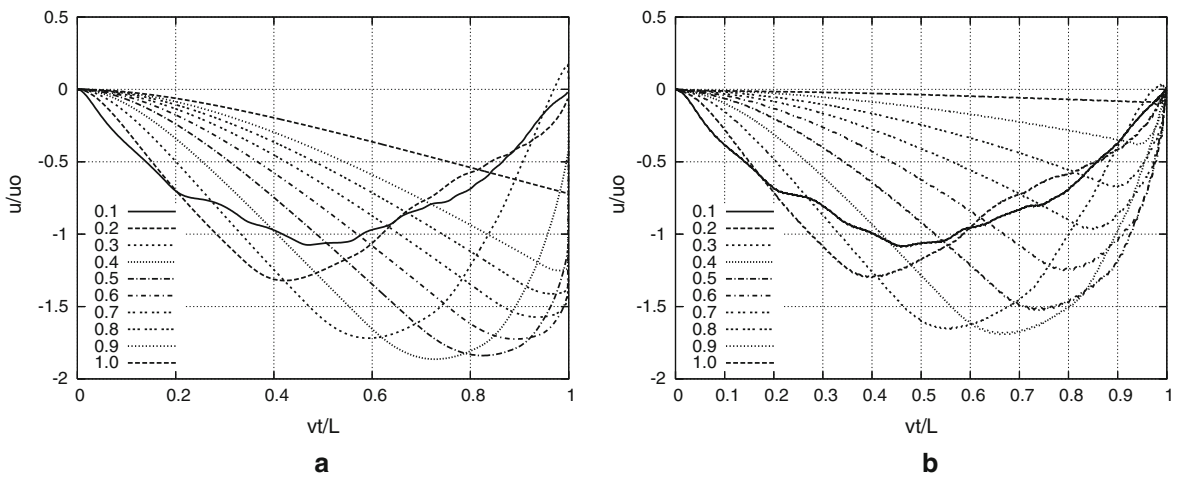

Fig. 3 Displacements computed analytically–numerically with Eq. (5) at various speed (**a**) and numerical analysis with moving spring-mass system (**b**)

3 Space-time finite element approach

The numerical analysis of the problem of the moving inertial load is performed with the use of the space-time finite element method. We can mention that attempts to the classical finite element solution failed.

3.1 Discretization of the string

We consider Eq. (1) in the space-time domain $\Omega = \{(x,t)\colon 0 \le x \le b, \quad 0 \le t \le h\}$. The equation of the virtual power is obtained by multiplying (1) by the virtual velocity $v^*(x,t)$. The total virtual power in Ω is equal to

$$\int_0^h \int_0^b v^*(x,t) \left(\rho A \frac{\partial^2 u}{\partial t^2} - N\frac{\partial^2 u}{\partial x^2} - \eta \frac{\partial u}{\partial t}\right) \mathrm{d}x\, \mathrm{d}t = 0. \tag{10}$$

η denotes internal damping coefficient. Node numbering in the space-time element is presented in Fig. 5. Integrating (10) by parts with respect to x results in

$$\rho A \iint_\Omega v^* \frac{\partial v}{\partial t}\, \mathrm{d}\Omega + N \iint_\Omega \frac{\partial v^*}{\partial x}\frac{\partial u}{\partial x}\, \mathrm{d}\Omega - \eta \iint_\Omega v^* v\, \mathrm{d}\Omega = 0. \tag{11}$$

We assume linear variation of velocity $v = \partial u/\partial t$ within x and t:

$$v(x,t) = \sum_{i=1}^{4} N_i(x,t)\, v_i. \tag{12}$$

In the domain Ω the shape function $\mathbf{N} = [N_1, \ldots, N_4]$ has the form

$$\mathbf{N} = \left[\frac{1}{bh}(x-b)(t-h), \quad -\frac{1}{bh}x(t-h), \quad -\frac{1}{bh}(x-b)t, \quad \frac{1}{bh}xt\right]. \tag{13}$$

Displacements are computed from the velocity equation by integration

$$u(x,t) = u(x,0) + \int_0^t (N_1 v_1 + \cdots + N_4 v_4)\, \mathrm{d}t = u(x,0) + \int_0^t \mathbf{N}^* \mathbf{v}\, \mathrm{d}t. \tag{14}$$

Finally, we have

$$u(x,t) = u(x,0) + \frac{xt^2}{2bh}(v_1 - v_2 - v_3 + v_4) + \frac{xt}{b}(-v_1 + v_2) + \frac{t^2}{2h}(-v_1 + v_3) + v_1 t. \tag{15}$$

Derivative $\partial u/\partial x$ can also be computed

$$\partial u/\partial x = \frac{t^2}{2bh}(v_1 - v_2 - v_3 + v_4) + \frac{t}{b}(-v_1 + v_2) + \left.\frac{\mathrm{d}u}{\mathrm{d}x}\right|_{t=0}. \tag{16}$$

The proper choice of virtual functions v^* is a fundamental question of the space-time approach. Different functions result in solution schemes of different properties: accuracy and stability. We propose a simple form with distribution δ in $t = \alpha h$ (Fig. 4a).

$$v^*(x,t) = \delta(t - \alpha h)\left[\left(1 - \frac{x}{b}\right) v_3 + \frac{x}{b}\, v_4\right]. \tag{17}$$

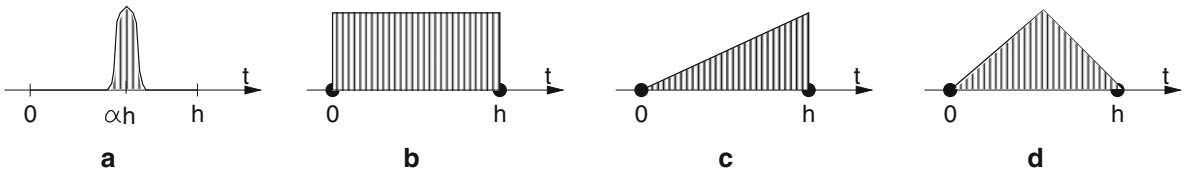

Fig. 4 Virtual functions: **a** delta Dirac shape, **b** hat shape, **c** triangle shape, **d** roof shape

Required derivatives of virtual v^* and real v functions can be determined from (17) and (12)

$$\frac{\partial v^*}{\partial x} = \frac{1}{b}(-v_3 + v_4), \tag{18}$$

$$\frac{\partial v}{\partial t} = \frac{x}{bh}(v_1 - v_2 - v_3 + v_4) + \frac{1}{h}(-v_1 + v_3). \tag{19}$$

We notice that the Dirac δ term in the subintegral function reduces the integration in Ω to the integration over $0 \le x \le b$. Finally, the Eq. (11) can be written in the following matrix form:

$$\begin{aligned}
&\left\{ \rho A \int_0^b \begin{bmatrix} -\left(\frac{x}{b} - 1\right) \\ \frac{x}{b} \end{bmatrix} \left[\frac{x}{bh} - \frac{1}{h},\ -\frac{x}{bh},\ -\frac{x}{bh} + \frac{1}{h},\ \frac{x}{bh} \right] \mathrm{d}x \right. \\
&+ N \int_0^b \begin{bmatrix} -\frac{1}{b} \\ \frac{1}{b} \end{bmatrix} \left[\frac{t^2}{2bh} - \frac{t}{b},\ -\frac{t^2}{2bh} + \frac{t}{b},\ -\frac{t^2}{2bh},\ \frac{t^2}{2bh} \right] \mathrm{d}x \Big|_{t=\alpha h} + N \int_0^b \begin{bmatrix} -\frac{1}{b} \\ \frac{1}{b} \end{bmatrix} \varepsilon_0 \mathrm{d}x \\
&\left. - \eta \int_0^b \begin{bmatrix} -(\frac{x}{b} - 1) \\ \frac{x}{b} \end{bmatrix} \left[\frac{(x-b)(t-h)}{bh},\ -\frac{x(t-h)}{bh},\ -\frac{(x-b)t}{bh},\ \frac{xt}{bh} \right] \mathrm{d}x \Big|_{t=\alpha h} \right\} \begin{Bmatrix} v_1 \\ \vdots \\ v_4 \end{Bmatrix} = 0.
\end{aligned} \tag{20}$$

The resulting matrices are as listed below:

$$\mathbf{M} = \frac{\rho b}{h} \left[\begin{array}{cc|cc} -\frac{1}{3} & -\frac{1}{6} & \frac{1}{3} & \frac{1}{6} \\ -\frac{1}{6} & -\frac{1}{3} & \frac{1}{6} & \frac{1}{3} \end{array} \right] = \frac{1}{h} [-\mathbf{M}_s \mid \mathbf{M}_s] \tag{21}$$

$$\begin{aligned}
\mathbf{K} &= \frac{Nh}{b} \left[\begin{array}{cc|cc} \alpha(1-\frac{\alpha}{2}) & -\alpha(1-\frac{\alpha}{2}) & \frac{\alpha^2}{2} & -\frac{\alpha^2}{2} \\ -\alpha(1-\frac{\alpha}{2}) & \alpha(1-\frac{\alpha}{2}) & -\frac{\alpha^2}{2} & \frac{\alpha^2}{2} \end{array} \right] \\
&= h \left[\alpha(1 - \frac{\alpha}{2}) \mathbf{K}_s \mid \frac{\alpha^2}{2} \mathbf{K}_s \right]
\end{aligned} \tag{22}$$

$$\mathbf{C} = \eta b \left[\begin{array}{cc|cc} \frac{1-\alpha}{3} & \frac{1-\alpha}{6} & \frac{\alpha}{3} & \frac{\alpha}{6} \\ \frac{1-\alpha}{6} & \frac{1-\alpha}{3} & \frac{\alpha}{6} & \frac{\alpha}{3} \end{array} \right] = [(1-\alpha)\mathbf{C}_s \mid \alpha \mathbf{C}_s] \tag{23}$$

M, **K**, and **C** are the space-time inertia, stiffness and viscous damping matrices, respectively. We notice that they are composed of two square matrices, each of a dimension equal to the number of degrees of freedom in a spatial finite element. Matrices $\mathbf{M_s}$, $\mathbf{K_s}$, and $\mathbf{C_s}$ have the same or similar form to respective matrices derived traditionally from the classical finite element approach. The third term of Eqn. (20) expresses nodal forces **e** in the beginning of the time step t_0. ε_0 is the strain at t_0. The final form of the motion equation establishes the force equilibrium on the edge of the element domain Ω. Vector **v** contains nodal velocities $\mathbf{v}_i$ at the initial time $t = t_i$ and $\mathbf{v}_{i+1}$ at the final time $t = t_i + h$.

$$(\mathbf{M} + \mathbf{C} + \mathbf{K}) \begin{Bmatrix} \mathbf{v}_i \\ \mathbf{v}_{i+1} \end{Bmatrix} + \mathbf{e} = \mathbf{0} \quad \text{or} \quad \mathbf{K}^* \mathbf{v} + \mathbf{e} = \mathbf{0}. \tag{24}$$

The velocity vector $\mathbf{v}_{i+1}$ is the only unknown vector in the above step-by-step equation. Finally, we must compute displacements $\mathbf{q}_{i+1}$. We use the formula

$$\mathbf{q}_{i+1} = \mathbf{q}_i + h[\beta \mathbf{v}_i + (1-\beta) \mathbf{v}_{i+1}] \tag{25}$$

The stability analysis results in $\beta = 1 - \alpha$.

3.2 Discretization of the string element carrying moving mass

The last term $\delta(x - v_m t)\, m\, \mathrm{d}^2u(v_m t, t)/\mathrm{d}t^2$ in the motion Eq. (1) describes the inertial moving mass. $\mathrm{d}^2u(v_m t, t)/\mathrm{d}t^2$ is the vertical acceleration of the moving mass and at the same time the acceleration of the point of the string in which the mass is temporarily placed (it is $x = x_0 + v_m t$). The acceleration of the mass $\mathrm{d}^2u(v_m t, t)/\mathrm{d}t^2$ moving with a constant velocity v_m, according to the Renaudot formula (which in fact is the chain rule of differentiation), results in three terms

$$\frac{\mathrm{d}^2u(v_m t, t)}{\mathrm{d}t^2} = \left.\frac{\partial^2 u(x,t)}{\partial t^2}\right|_{x=v_m t} + 2v_m \left.\frac{\partial^2 u(x,t)}{\partial x \partial t}\right|_{x=v_m t} + v_m^2 \left.\frac{\partial^2 u(x,t)}{\partial x^2}\right|_{x=v_m t}. \tag{26}$$

Thus, we can separate the transverse acceleration, the Coriolis acceleration, and the centrifugal acceleration, respectively. This is the so-called Renaudot notation for the constant speed v_m. Another one, the so-called Jakushev notation (or approach) finally gives the same result in our case of the constant mass m.

In our space-time finite element method we formulate equations in terms of velocities. The mass acceleration $\frac{\mathrm{d}^2u(v_m t,t)}{\mathrm{d}t^2}$ is expressed in terms of velocities as well

$$\begin{aligned}\frac{\mathrm{d}^2}{\mathrm{d}t^2}u(x_0 + v_m t, t) &= \frac{\mathrm{d}}{\mathrm{d}t}\left(\left.\frac{\partial u(x,t)}{\partial t}\right|_{x=x_0+v_m t} + v_m \left.\frac{\partial u(x,t)}{\partial x}\right|_{x=x_0+v_m t}\right)\\ &= \frac{\mathrm{d}}{\mathrm{d}t}\left(V(x,t)|_{x=x_0+v_m t}\right) + v_m \frac{\mathrm{d}}{\mathrm{d}t}\left(\left.\frac{\partial u(x,t)}{\partial x}\right|_{x=x_0+v_m t}\right)\\ &= \left.\frac{\partial V(x,t)}{\partial t}\right|_{x=x_0+v_m t} + v_m \left.\frac{\partial V(x,t)}{\partial x}\right|_{x=x_0+v_m t} + v_m \frac{\mathrm{d}}{\mathrm{d}t}\left(\left.\frac{\partial u(x,t)}{\partial x}\right|_{x=x_0+v_m t}\right)\end{aligned} \tag{27}$$

The first term represents the transversal acceleration. The second term defines the Coriolis acceleration. The third term is integrated over time and it results in the centrifugal acceleration, contributed in the matrix $\mathbf{K_m}$ and nodal forces $\mathbf{e}$.

In the final stage three resulting matrices are responsible for transverse inertia (the matrix has the form of the inertia matrix), damping forces (the matrix multiplied by the velocity vector has a form similar to the Coriolis forces) and stiffness (potential) forces (the matrix, if multiplied by the velocity vector, has a form similar to the centrifugal forces). The third matrix appears as a result of initial displacements in the time interval.

Let us now follow this idea and treat numerically the right-hand side inertial term of (1). The same mathematical steps as in the case of pure string enables us to integrate the inertial term

$$\int_0^h \int_0^b \mathbf{N}^* m \delta(x - v_m t) \frac{\mathrm{d}^2u(x_0 + v_m t, t)}{\mathrm{d}t^2}\, \mathrm{d}x, \mathrm{d}t. \tag{28}$$

We consider first the integral term of (14). We use the same linear interpolation of the velocity (12). The virtual velocity v^*:

$$v^*(x,t) = \mathbf{N}^* \dot{\mathbf{q}}_p = \delta(t - \alpha h) \begin{bmatrix} 1 - \frac{x}{b} \\ \frac{x}{b} \end{bmatrix} \dot{\mathbf{q}}_p \tag{29}$$

Consequent integration results in two matrices: the moving mass inertia matrix $\mathbf{K}_m$

$$\mathbf{M}_m = \frac{m}{h}\left[\begin{array}{cc|cc} -(1-\kappa)^2 & -\kappa(1-\kappa) & (1-\kappa)^2 & \kappa(1-\kappa) \\ -\kappa(1-\kappa) & -\kappa^2 & \kappa(1-\kappa) & \kappa^2 \end{array}\right], \tag{30}$$

where $\kappa = (x_0 + v_m \alpha h)/b$, x_0 is a starting position of the mass in the space-time element (at $t = t_0$) (see Fig. 5), and the moving mass damping matrix $\mathbf{C}_m$

$$\mathbf{C}_m = \frac{mv}{b}\left[\begin{array}{cc|cc} -(1-\kappa)(1-\beta) & (1-\kappa)(1-\beta) & -(1-\kappa)\beta & (1-\kappa)\beta \\ -\kappa(1-\beta) & \kappa(1-\beta) & -\kappa\beta & \kappa\beta \end{array}\right]. \tag{31}$$

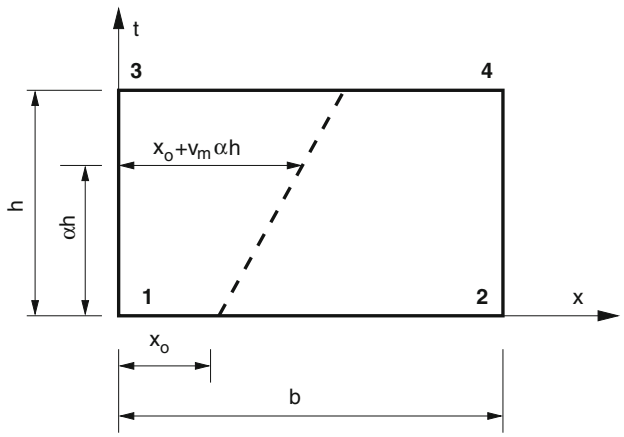

Fig. 5 Mass path in the space-time finite element

Since displacements of the left and right node of the element are expressed by $u_L = u_L^0 + h[\beta v_1 + (1-\beta)v_3]$ and $u_R = u_R^0 + h[\beta v_2 + (1-\beta)v_4]$, we can derive the required $\mathrm{d}u_0/\mathrm{d}x$

$$\frac{\mathrm{d}u_0}{\mathrm{d}x} = \frac{u_R - u_L}{b} = \frac{u_R^0 - u_L^0}{b} + \frac{h}{b}[-\beta v_1 + \beta v_2 - (1-\beta)v_3 + (1-\beta)v_4] \tag{32}$$

Matrix $\mathbf{K}_\mathrm{m}$ is the stiffness mass matrix

$$\mathbf{K}_\mathrm{m} = \frac{hmv_m^2}{b^2}\left[\begin{array}{cc|cc} \beta & -\beta & 1-\beta & -(1-\beta) \\ -\beta & \beta & -(1-\beta) & 1-\beta \end{array}\right] \tag{33}$$

The term $(u_R^0 - u_L^0)/b$ in (32) multiplied by mv^2/b results in initial nodal forces $\mathbf{e}$ in the space-time layer (24).

We can mention here that the hat-shaped virtual function results in the different stiffness matrix of the string element

$$\mathbf{K} = \frac{Nh}{b}\left[\begin{array}{cc|cc} 1/3 & -1/3 & 1/6 & -1/6 \\ -1/3 & 1/3 & -1/6 & 1/6 \end{array}\right] = h\left[\frac{1}{3}\mathbf{K}_s \;\middle|\; \frac{1}{6}\mathbf{K}_s\right], \tag{34}$$

and the string element carrying the mass $\mathbf{K}_m$

$$\mathbf{K}_m = \frac{hmv_m^2}{b^2}\left[\begin{array}{cc|cc} 1/6 & -1/6 & 1/3 & -1/3 \\ -1/6 & 1/6 & -1/6 & 1/3 \end{array}\right] \tag{35}$$

We can compare both matrices with (22) and (33).

3.3 Discretization of the beam element carrying moving mass

We consider here the Bernoulli–Euler model of a beam. The motion of the Bernoulli–Euler beam under the moving mass is described by the equation

$$EI\frac{\partial^4 u(x,t)}{\partial x^4} + \rho A\frac{\partial^2 u(x,t)}{\partial t^2} = \delta(x - v_m t)P - \delta(x - v_m t)m\frac{\mathrm{d}^2 u(v_m t, t)}{\mathrm{d}t^2}, \tag{36}$$

with boundary conditions

$$u(0,t) = 0, \quad u(l,t) = 0, \quad \left.\frac{\partial^2 u(x,t)}{\partial x^2}\right|_{x=0} = 0, \quad \left.\frac{\partial^2 u(x,t)}{\partial x^2}\right|_{x=l} = 0 \tag{37}$$

and initial conditions

$$u(x,0) = 0, \quad \left.\frac{\partial u(x,t)}{\partial t}\right|_{t=0} = 0. \tag{38}$$

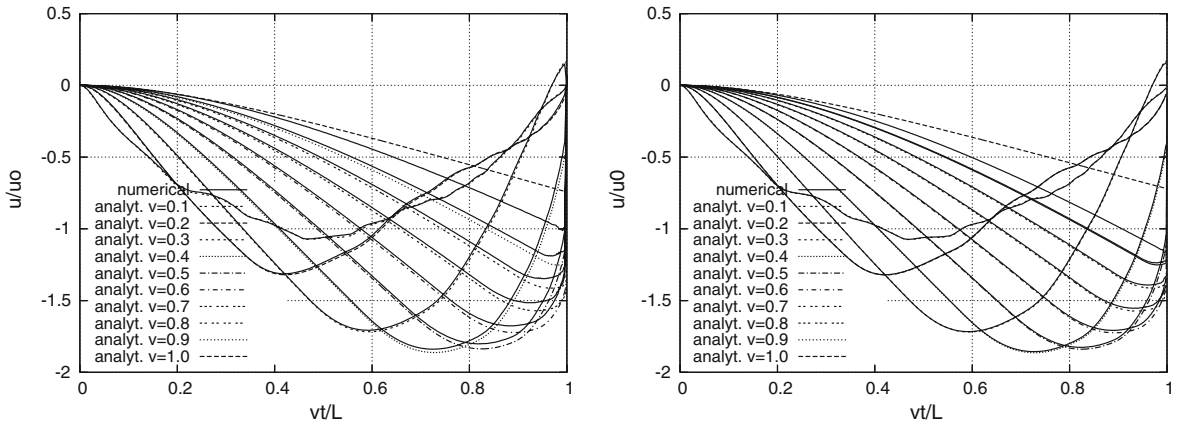

Fig. 6 Displacements under the moving mass—space-time finite element solution for a virtual Dirac function with $\alpha = 0.5$ (*left*) and a virtual hat function (*right*) compared with analytical solution

Characteristic matrices are derived in a classical way. In the element carrying the mass we substitute the derivative $\mathrm{d}^2 u(v_m t, t)/\mathrm{d}t^2$ in the equation of the virtual power by three terms obtaind from the chain rule derivation (26). They contribute vertical inertial, centrifugal, and Coriolis forces. The choice of the virtual function is the crucial point in this stage. Matrices derived with the hat-shaped function give excellent accuracy of results. In the case of the Timoshenko beam, we follow the same way as in the case of the Bernoulli–Euler beam.

4 Numerical results

Numerical results obtained with the proposed space-time approach can be compared with the analytical solution. Moreover, the spring-mass finite element solution can also be plotted. In our tests the string was discretized by a set of 200 finite elements. The time step h was equal to $b/40v_m$. It means that the mass passes from joint to joint in 40 time steps. Results obtained by the space-time finite element method are presented in Fig. 6.

Further examples prove the efficiency and accuracy of the approach. One can plot the displacements of selected fixed points of the string. In such a case the results exhibit very good coincidence with the analytical-numerical approach.

We can attach only for information the plot of oscillator displacements moving over the span. Two separate systems were considered: a string subjected to a contact force between the oscillator spring and the string, and the oscillator itself, subjected to a force P applied to a mass and displacements determined from the string motion, applied to a spring. The oscillator spring stiffness was assumed to be high enough, to simulate a rigid contact of the mass with the string. We notice that the solution is significantly worse (Fig. 3b) than results obtained with the method presented in this paper. Numerical results of displacements in time of the Bernoulli–Euler beam are presented in Fig. 7. The following data were applied: $E = 1.0$, $A = 1.0$, $I = 0.01$, $l = 1.0$, $\rho = 1.0$, $m = 1.0$, and $P = 1.0$.

5 Conclusions

In this paper we dealt with numerical analysis of the string vibrations under the moving inertial load. We derived the matrix formula of the time integration procedure on the base of the space-time finite element method. Solutions presented in the literature are derived with classical time integration schemes. Results published in references cannot be accepted. In common engineering practice the massless force acting on the string in the form of oscillator is applied. Such results are greatly underestimated and for the velocity higher than 0.2–0.3 of the critical speed cannot be taken into account.

The numerical approach presented in this paper can be applied in the wide range of the speed and also in the critical and over-critical range. The precision of results is high. In the case of the speed higher than the wave speed in strings, the particle's trajectory does not differ from the theoretical zero line. Discontinuities at $x = l$ exhibited and proved analytically in literature are reflected in figures presenting numerical trajectories.

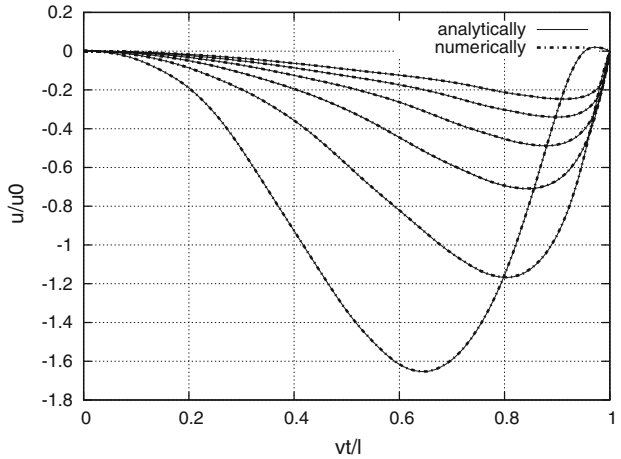

Fig. 7 Displacements under the mass moving on the Barnoulli–Euler beam

Displacements of beams, both Bernoulli–Euler and Timoshenko type, obtained numerically and semi-analytically, perfectly coincide.

The method presented in this paper can be successfully applied to other structures subjected to inertial load, for example frames and plates. The space-time finite element approach shows the way for the classical numerical solution of the moving mass problem with the Newmark method. Unfortunately, nowadays, the space-time approach is the only efficient solution.

References

1. Filho, F.V.: Finite element analysis of structures under moving loads. Shock Vibr. Dig. **10**(8), 27–35 (1978)
2. Bajer, C.: Space-time finite element formulation for the dynamical evolutionary process. Appl. Math. Comp. Sci. **3**(2), 251–268 (1993)
3. Bajer, C.I.: Triangular and tetrahedral space-time finite elements in vibration analysis. Int. J. Numer. Meth. Eng. **23**, 2031–2048 (1986)
4. Bajer, C.I.: Notes on the stability of non-rectangular space-time finite elements. Int. J. Numer. Meth. Eng. **24**, 1721–1739 (1987)
5. Bajer, C.I., Bohatier, C.: The soft way method and the velocity formulation. Comput. Struct. **55**(6), 1015–1025 (1995)
6. Bajer, C.I.: Adaptive mesh in dynamic problem by the space-time approach. Comput. Struct. **33**(2), 319–325 (1989)
7. Bajer, C.I., Bogacz, R., Bonthoux, C.: Adaptive space-time elements in the dynamic elastic-viscoplastic problem. Comput. Struct. **39**, 415–423 (1991)
8. Bajer, C.I.: Dynamics of contact problem by the adaptive simplex-shaped space-time approximation. J. Theor. Appl. Mech. **7**, 235–248. Special issue, suplement no. 1 (1988)
9. Bajer, C.I.: The space-time approach to rail/wheel contact and corrugations problem. Comp. Assoc. Mech. Eng. Sci. **5**(2), 267–283 (1998)
10. Bohatier, C.: A large deformation formulation and solution with space-time finite elements. Arch. Mech. **44**, 31–41 (1992)
11. Stokes, G.G.: Discussion of a differential equation relating to the breaking railway bridges. Trans. Cambridge Philosoph. Soc., Part **5**, 707–735 (1849). Reprinted in: Mathematical and Physical Papers, Cambridge, vol. II, pp. 179–220 (1883)
12. Frỳba, L.: Vibrations of Solids and Structures under Moving Loads. Thomas Telford House, New York (1999)
13. Dyniewicz, B., Bajer, C.I.: Inertial load moving on a string—discontinuous solution. In: Szcześniak, W. (ed.) Theoretical Foundations in Civil Engineering, pp. 141–150. OWPW Warsaw (2007)
14. Dyniewicz, B., Bajer, C.I.: Paradox of the particle's trajectory moving on a string. Arch. Appl. Mech. (2008). doi:10.1007/s00419-008-0222-9